Facile "green" Aqueous Synthesis of Mono- And Bimetallic Trimesate Metal-Organic Frameworks

A. Nowacka, P. Briantais, C. Prestipino, F.X. Llabrés I Xamena

Facile "green" aqueous synthesis of mono- and bimetallic trimesate metal-organic frameworks

Anna Nowacka,[a] Pol Briantais,[b] Carmelo Prestipino[b,*] and Francesc X. Llabrés i Xamena[a,*]

[a] *Instituto de Tecnología Química, Universitat Politècnica de València, Consejo Superior de Investigaciones Científicas, Avda. de los Naranjos, s/n, 46022 Valencia, Spain*

[b] *Institut Sciences Chimiques de Rennes, UMR-CNRS 6226, Campus de Beaulieu, Université de Rennes 1, 35042 Rennes Cedex, France*

* Corresponding authors: fllabres@itq.upv.es
carmelo.prestipino@univ-rennes1.fr

ABSTRACT:

Various isoreticular mono- (Co^{2+}, Ni^{2+}, Cu^{2+} and Zn^{2+}) and bimetallic (Co-Ni, Co-Zn, Mn-Ni) trimesate MOFs have been prepared by a fast (10 minutes) and green synthesis method from aqueous solutions, at room temperature and ambient pressure. A combined XRD and SEM/EDX analysis clearly revealed that bimetallic compounds for true solid solutions rather than a simple physical mixture of pure phase monometallic compounds. Moreover, a detailed evaluation of the evolution of cell parameters with the composition provides strong evidences indicating a preferential occupation of one crystallographic position (bidentate terminal sites) by Co^{2+} (or Mn^{2+}) ions. This leads to a precise and predictable array of metal ions in the framework, which can be finely tuned by changing the overall composition of the bimetallic MOF. Implications are envisaged in the design and catalytic properties of well-defined single-site catalysts.

INTRODUCTION:

In the last two decades, metal organic frameworks (MOFs) have attracted a great deal of attention due to their potential applications in several areas, including heterogeneous catalysis.[1-3] This is due to the huge variability of chemical compositions and pore architectures attainable with these materials, along with extremely large surface areas and pore volumes, and the possibility to introduce new functionalities in preformed MOFs through post-synthesis methods[4]. This provides an unprecedented level of tunability of the MOF composition, hardly found in any other family of porous crystalline solids. Among the many possibilities offered by MOFs, isoreticular compounds can be prepared having the same topology and pore architecture but containing different ligands[5-6] and/or metals ions[7] in the structure. For instance, replacing one metal ion by another in the inorganic building units provides a way to fine tune the chemical properties of these compounds, such as acid-base[8] and redox properties[9]. Additionally, bimetallic MOFs can also be prepared, either by direct synthesis or through post-synthesis modification, in which the second metal type can either modulate the properties of the other metal ions in the MOF, or it can introduce totally new functionalities not present in the pristine compound. It is even possible to combine in just one compound different activities arising from the individual metal ions, so that multifunctional MOFs can readily be prepared to be used in multi-step one pot transformations[10].

In spite of the high potential of MOFs, their synthesis procedure is most often one of the main drawbacks hindering their large scale industrial application. Most of the MOFs described so far are usually prepared in DMF or other organic solvents, which can be toxic and/or dangerous to handle. Moreover, many MOFs require the use of non-commercial and/or expensive organic ligands, which introduce additional synthesis steps and rise up the final price of the catalyst, thus hampering the large-scale synthesis of these MOFs and making the resulting materials less economically appealing, as compared to cheaper alternative catalysts. The use of high synthesis temperatures (100-200ºC in many cases), overpressures, and long synthesis times (one week or longer in certain cases) are also undesired characteristics of most existing MOF preparations described so far. It is thus evident that new, greener and easily scalable synthetic procedures of "cheap" MOFs need to be developed to facilitate their transfer to the industrial scale production[11-14]. Ideally, these synthetic procedures should avoid the use of organic solvents (water is the preferred solvent), should be carried out at room temperature and atmospheric pressure, and using commercial, cheap and largely available organic ligands. Recently, interesting progress has been

done on solvent-free[15-17] and liquid-assisted mechanochemical MOF synthesis[18-20], as well as continuous flow synthesis at the gram and multigram scale[21], which represent significant steps in the future of "green" and industrial friendly synthesis of MOFs in a more sustainable way.

Following the aforementioned indications, in the present work we have applied a "green" aqueous synthesis procedure to prepare a series of trimesate MOFs in high yields, at room temperature, ambient pressure and very short time (10 minutes). Herein, we will show that the method can be used to prepare various monometallic divalent compounds, as well as bimetallic compounds of different compositions. In the latter case, we will demonstrate that true solid solutions are formed, in which both metal ions distribute homogeneously throughout the whole crystal.

EXPERIMENTAL SECTION:

All reagents were of analytical grade and used as received without further purification.

Powder material preparation. All materials were prepared by "green", water based synthesis procedure at room temperature and ambient pressure. First, a 0,1M Na_3BTC stock solution (BTC = 1,3,5-benzene tricarboxylate) was prepared by dissolving 30 mmol of NaOH and 10 mmol of 1,3,5-benzenetricarboxylic acid in 100 mL of distilled water under vigorous stirring. Consequently, the MOFs were obtained by mixing together under rapid stirring 3 mmol of metal salt precursor (Co, Ni, Zn, Cu, or its mixture in appropriate ratio) and 20 mL of the Na_3BTC 0,1M(aq) solution (2 mmol). Optionally, 10 mL of ethanol absolute was also added to the above solution. Stirring was continuing at room temperature and ambient pressure for the next 10 min. The solid obtained was separated by centrifugation and carefully washed with distilled water (3x) and ethanol (1x). The resulting powder materials where let to dry in air at room temperature.

Single crystal materials preparation. Starting from the above stock 0,1M Na_3BTC aqueous solution, a 1:8 dilution was obtained, resulting in a Na_3BTC 0.0125M solution. For the preparation of monometallic compounds, a 0,1M aqueous solution of the corresponding metal precursor was prepared and placed inside a test tube. In the second step, Na_3BTC 0,0125M solution was added carefully to the solution in the tube using a syringe (sliding down the walls of the tube). As prepared solutions were left overnight for crystallization. Obtain single crystals were carefully washed with water and dried in air at room temperature. For the preparation of bimetallic compounds, the Ni

0,1M and Co 0,1M solutions were mixed with water in proper ratio, giving "Ni/Co solution" (see Table S1 in the Supporting Information) and placed inside the test tube, and treated likewise.

Powder XRD characterization. Powder M-BTC materials synthetized by water solution were characterized by X-ray powder diffraction (XRPD) using a Bruker AXS D8 Advance diffractometer equipped with a primary Ge (111) Johansson monochromator (selecting Cu Kα1 radiation) and a mono-dimensional detector Lynxeye. In the case of CoBTC, in order to reduce low signal to noise ratio induced by Co fluorescence, the electronic windows for photon acceptance has been reduced and counting time increased to obtain comparable patterns to the others materials.

Structure determination of powder materials. The crystal structure for monometallic materials has been confirmed by Rietveld refinement of the diagrams so obtained, applying rigid body constrain to the carbon atoms of BTC molecule, using the software Jana[22]. During minimization, atomic positions and thermal parameters with isotropic profile parameters describing instrumental broadening, size and strain effect were refined. Thermic parameters were considered isotropic for all atoms, and constrained to be the same for each chemical species. It is worth to note that although the quality of fit is sufficient to clarify the structure, few negative thermal parameters are present in the final refinement probably due to the difficulty to discriminate between close elements in X-ray diffraction and the relatively higher error associated with the scattering of light elements (C,O). For bi-metallic material series, in order to obtain the most precise cell parameters determinations the diagrams were analyzed by Le Bail refinement[23] as implemented in the Fullprof code[24]. Such approach allows to fully de-correlate atomic parameters from cell metrics and to avoid possible systematic errors induced by an approximate estimation of reflection intensity. Errors on the fitting parameters have been corrected by Berar factors[25].

Single crystal XRD characterization. Data collections were performed at low temperature (T = 100(2) K) using an APEXII Bruker-AXS diffractometer and Mo-Kα radiation (λ = 0.71073 Å). Several single crystals were tested in order to check their quality and that there was no allotropic phase. Each time, they were mounted on a cryoloop with the help of Paraton grease.

Structure determination of single crystal materials. The structure was solved by dual-space algorithm using the SHELXT program[26], and then refined with full-matrix least-square methods (SHELXL)[27] with the aid of the Olex2 interface[28]. All non-hydrogen atoms were refined with anisotropic atomic displacement parameters. H atoms were finally included in their calculated positions. Further details of refinement are available in the CIF files.

Microscopy characterization. Morphology and element mapping of the single crystal samples, were analyzed with a field emission scanning electron microscope (FESEM) model JEOL 7001F, equipped with a spectrometer of energy dispersion of X-ray (EDX) form Oxford Instruments.

RESULTS AND DISCUSSION:

The generic synthesis method used in this work is schematically shown in Fig. 1. Briefly, an aqueous solution of trisodium benzene-1,3,5-tricarboxylate (Na_3BTC) was poured onto a suitable divalent metal salt solid precursor at room temperature under vigorous stirring. The amounts of Na_3BTC solution and metal precursor used were adjusted to have a 2:3 molar ratio. Optionally, a small volume of ethanol can also be added to the above mixture, which was shown to accelerate the precipitation of the MOF and to increase the final yield obtained, which is typically higher than 90% in all cases. Stirring of the mixture was continued for 10 minutes, and the solid obtained was separated by centrifugation and carefully washed with distilled water (three times) and ethanol (once). Finally, the powder so obtained was air-dried overnight at room temperature.

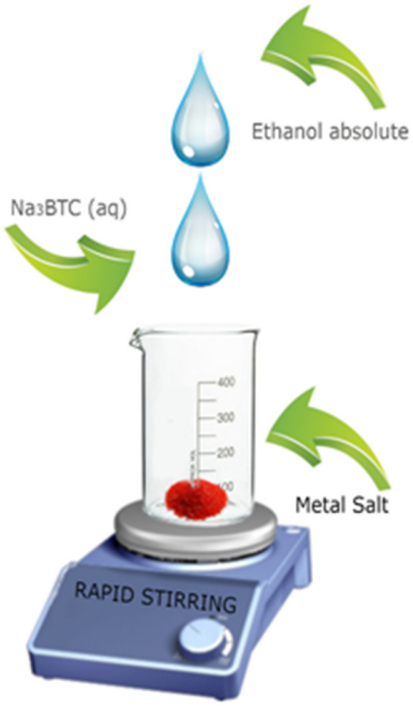

Figure 1. Aqueous synthesis of MOFs is carried out at room temperature and atmospheric pressure within 10 minutes.

As it can be observed, the above method has a series of advantages that improve the green credentials, sustainability and industrial feasibility of the MOF preparation: synthesis from non-toxic water solutions, room temperature and atmosphere pressure, very short synthesis time (~ 10 min.), high yield, easy separation and washing protocols, easily scalable method, and the use of a cheap and commercially available ligand precursor, H_3BTC. Also, the method tolerates a variety of metal salt precursors without producing appreciable changes in crystallinity of the final product, including nitrates, chlorides or sulfates, which are usually the preferred option for industry to minimize safety and corrosion issues[14].

Monometallic compounds

Various monometallic compounds were prepared following the method described above, and the solids were first characterized by powder diffraction (PXRD). MOFs containing Co^{+2}, Ni^{+2}, Cu^{+2} or Zn^{+2} were all found to be crystalline and isoreticular. In contrast, all our attempts to obtain an isoreticular Mn^{2+} compound were unsuccessful. The material obtained presented a clearly lower crystallinity and a different structure (see Fig. S1 in the Supporting Information). Hereafter, we will refer to these metal trimesate compounds as M-BTC, where M indicates the metal used in each case, though a more representative formula should be [μ-$M(H_2O)_{42}$(BTC)$M(H_2O)_4$BTC] (see below).

By comparing the XRD peak positions of the M-BTC materials with the existing MOF collected in the Cambridge Structure Database[29], the solids prepared with the above method were found to correspond to a family of metal trimesate compounds of general formula $M_3BTC_2 \cdot 12H_2O$, first synthetized by Yaghi and co-workers using a conventional solvothermal method[30]. This structural assignment was confirmed by Rietveld refinement of the synthetized M-BTC compounds, as shown in Fig. 2.

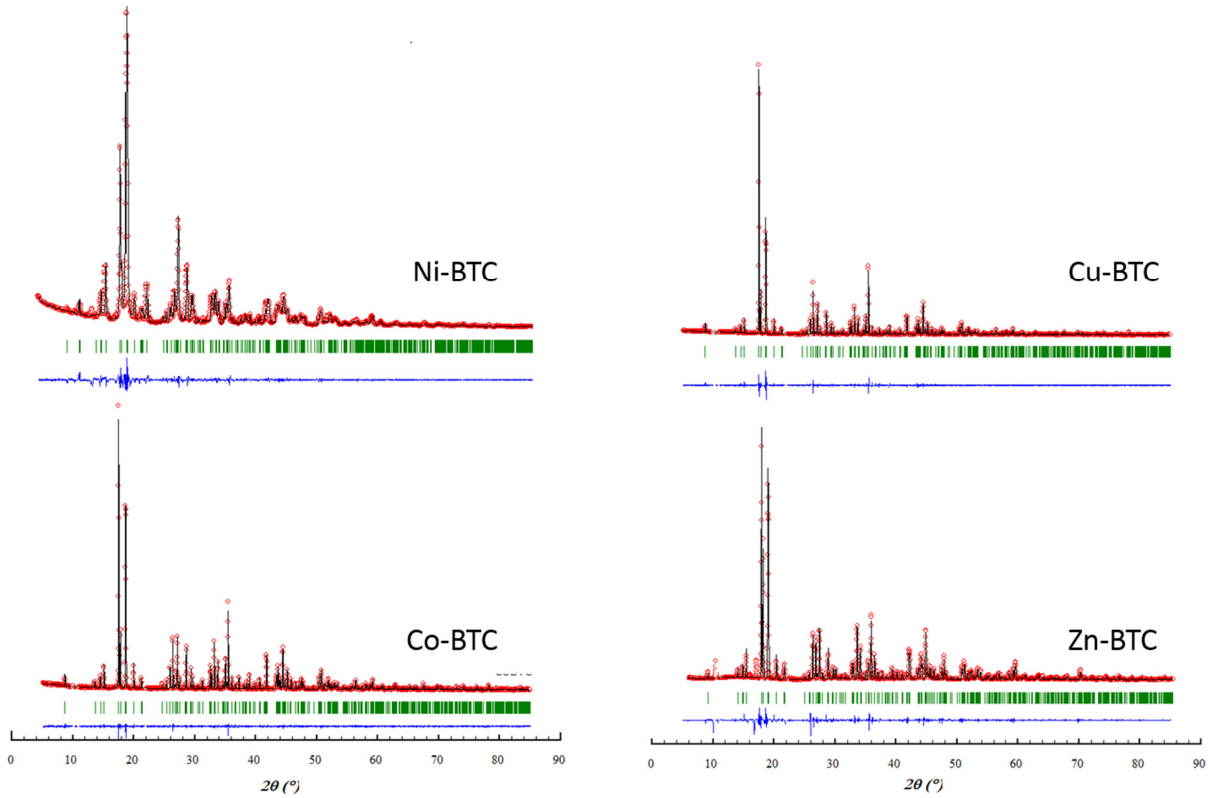

Figure 2. Rietveld refinement of XRD patterns: Observed (red dots), refined (black solid lines), and their difference (blue bottom line). Green vertical bars indicate the X-ray reflection positions.

Thermogravimetric curves of the M-BTC compounds (see Fig. S2 in the Supporting Information) typically showed two main steps at about 125-150 °C and 420-480 °C, corresponding to coordinated water and decomposition of the organic ligand, respectively. The observed weight losses were in agreement with the stoichiometry expected for a $M_3BTC_2 \cdot 12H_2O$ compound (see Table S2 in Supporting Information). In all cases, this stoichiometry was also in agreement with the corresponding ICP and elemental analysis (see Table S3 in Supporting Information).

$M_3BTC_2 \cdot 12H_2O$ compounds crystallize in the monoclinic *C*2 (5) space group with a layered structure whose cell metrics depends on the nature of the metal atom (see Table 1). The structure features infinite zigzag chains aligned along [101] direction that are formed by the alternation of BTC with M atoms. The repeating unit (black rectangle in Fig. 3) contains two types of M atoms, hereafter denoted bridging (Wyckoff position *4c*) and terminal (Wyckoff position *2b*), in a 2:1

ratio. Both BTC molecules in the repeating unit bind to bridging M atoms in an unidentate mode along the chain, and an additional M atom is coordinated in a bidentate fashion by one free carboxylate group on alternate BTC molecules. Individual zigzag chains stack along the *b* axis (Fig. 3b) to form layers in the (10-1) plane, while these layers are stacked along the *c* axis with an ABA arrangement (Fig. 3c and d). Interactions between chains are dominated by hydrogen bonds between water molecules of bridging and terminal M atoms, while interlayer interactions consist of hydrogen bonds between the carboxylate oxygens and the water molecule coordinated to both type of M atoms (see Fig. S3 in Supporting Information).

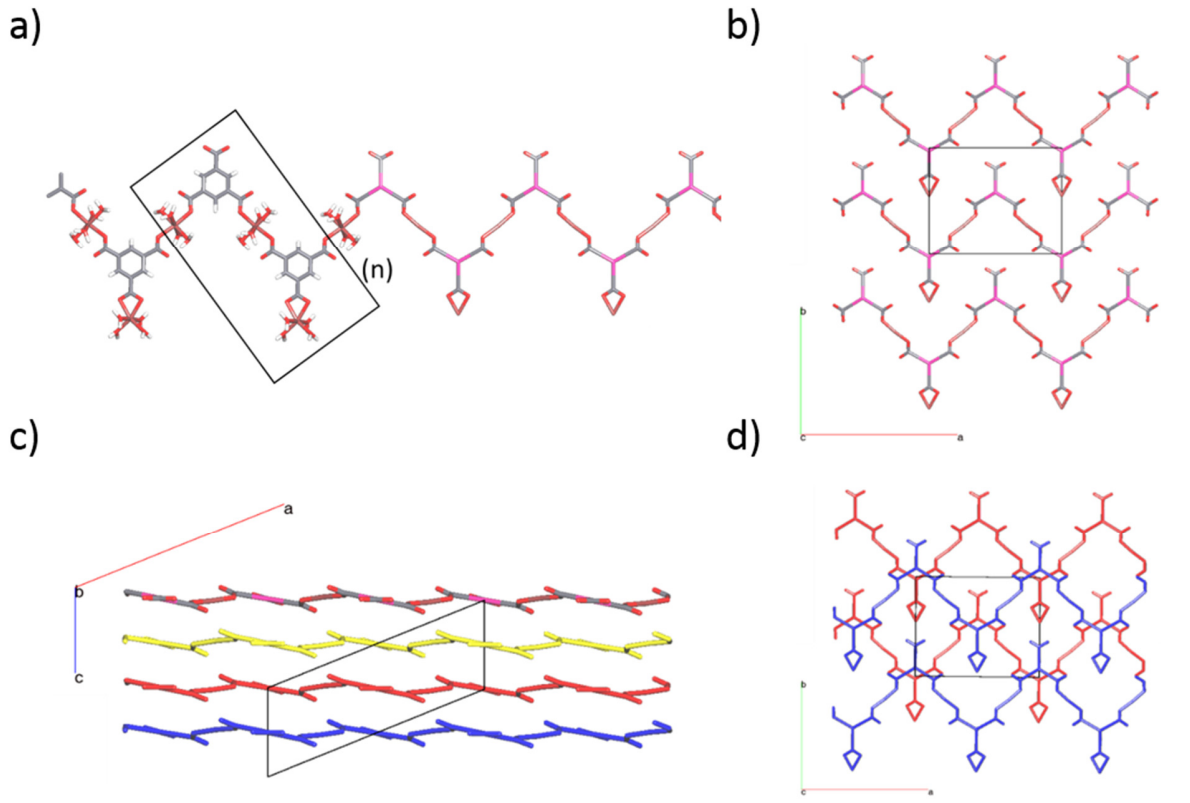

Figure 3. a) $M_3BTC_2 \cdot 12H_2O$ zigzag chains. The black rectangle single out the repeating unit. b) Single $M_3BTC_2 \cdot 12H_2O$ layer representation along (001) direction. Hydrogen atoms and water molecules have been removed for clarity. Cell borders are indicated by black lines. Layer packing representations along (001) and (010) directions are shown in parts c) and d) respectively. Chain are colored depending from the layer in which they lay.

Table 1. Cell metrics obtained by Le Bail refinement for monometallic trimesate MOFs.

Compound	Co-BTC	Ni-BTC	Cu-BTC	Zn-BTC
Space group	*C*2	*C*2	*C*2	*C*2
a (Å)	17.467(1)	17.440(7)	17.412(2)	17.475(6)
b (Å)	12.947(1)	12.867(9)	12.913(3)	12.926(5)
c (Å)	6.556(6)	6.539(6)	6.5669(2)	6.582(3)
β (°)	112.230(3)	112.603(4)	111.93(2)	112.443(4)
V (Å^3)	1372.53(3)	1354.91(7)	1369.63(5)	1374.30(6)
χ^2	1.62	1.35	1.45	1.78

In their original report on the hydrothermal synthesis of M-BTC compounds, Yaghi and co-workers studied the behavior of Co, Ni and Zn compounds upon thermal treatment and rehydration[30]. The authors concluded that the compounds showed a sequential loss of up to 11 water molecules out of the 12 present in the original hydrated solid. Although this partial dehydration process was accompanied by a severe loss of crystallinity and corresponding peak broadening, the structural order and crystallinity were reestablished upon exposure of the monohydrated compounds to water. A similar behavior was also observed for our compounds prepared at room temperature, as it is shown in Figure S4 for the Co-BTC compound. In this case, partial dehydration and rehydration of the solid is accompanied by a reversible color change from pink to blue and back to pink for the hydrated, partially dehydrated and rehydrated samples, respectively. These results demonstrate that the room temperature synthesis produces materials with a stability to the loss of guest molecules which is at least similar to that of the materials prepared at higher temperature.

Bimetallic compounds

Co-Ni bimetallic compounds. The above synthesis method was adapted to prepare different series of bimetallic compounds, including Co-Ni and Co-Zn mixtures. Thus, Co-Ni bimetallic trimesates with Co:Ni ratios in all the range of compositions were first prepared by mixing appropriate amounts of the two metal precursors with an aqueous Na_3BTC solution, as described in the Experimental Section. Hereafter, we will refer to these materials as CoxNi-BTC, in which x represents the (nominal) molar percentage of cobalt in the solid.

Powder XRD analysis confirmed that all the Co-Ni bimetallic materials were crystalline and isoreticular, as shown in Fig. S5 (Supporting Information). According to the ICP analysis (see Table S2 in Supporting Material), incorporation of both metals in the final solid was found to be quantitative with respect to the initial concentration of precursors used. Accordingly, a progressive color change of the samples with the composition was observed, passing from green (for the pure Ni-BTC) to pink (for pure Co-BTC), as shown in Fig. S6 (Supporting Information).

Since the pure monometallic compounds, Ni-BTC and Co-BTC, are both isoreticular with very similar cell parameters (see Table 1), one can expect that the isomorphous replacement of one metal by the other should be readily feasible without changing the framework structure of the MOF. However, due to the similar ionic radii and scattering factors of Ni^{2+} and Co^{2+}, it is not at all straightforward from the experimental point of view to discriminate whether a true solid solution or a simply physical mixture of the two monometallic MOFs is formed during the synthesis of the bimetallic samples. This is in general the case for the rest of bimetallic series prepared in the present work, which will be discussed later.

A first indication in favor of the formation of true solid solutions is that we did observe clear differences in the TGA curves of the bimetallic compounds and those corresponding to physical mixtures of the two pure Ni-BTC and Co-BTC, as shown in Fig. S7 in the Supporting Information. In particular, we note that in the case of the physical mixture there are two distinct weight losses associated to water (below 200ºC), corresponding to the two pure compounds, while only one water weight loss is seen in the Co30Ni-BTC solid solution. Likewise, the decomposition temperature of the solid solution and physical mixture are also clearly different, being around 70º higher for the solid solution.

Formation of solid solution is further supported by powder XRD. Indeed, we did not observe any peak splitting or the presence of new shoulders in the XRD patterns of the CoxNi-BTC samples, as could be expected for a physical mixture of the two monometallic MOFs. Moreover, the peaks of the bimentallic compounds are narrower than those of the pure Ni-BTC material (see insets in Fig. S5 in the Supporting Information). We observed definite shifts of the signals with the composition on going from pure Co-BTC to pure Ni-BTC, which clearly speaks in favor of a solid solution and against a simple physical mixture. To address this point in more detail, we have used Le Bail methods to extract the cell parameters from the corresponding powder XRD patterns of the compounds. The results obtained are shown graphically in Fig. 4.

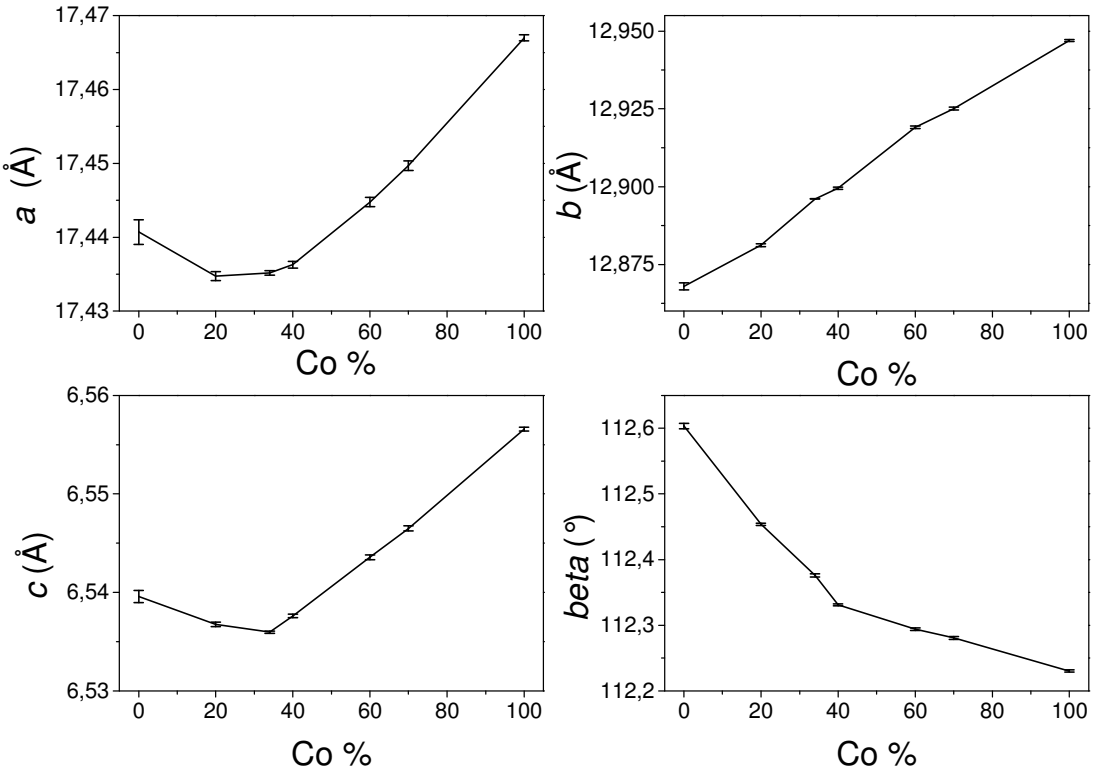

Figure 4. Variation of the cell parameters *a*, *b*, *c* and β, of bimetallic CoxNi-BTC compounds as a function of the molar composition.

As it can be observed, although the differences are relatively small, there is a continuous evolution of the cell parameters of CoxNi-BTC as a function of the composition, which follow different trends *for a, b c* and β. The observed variations in cell parameters are a consequence of the different complex interactions (mainly hydrogen bonding) between the carboxylate groups of the ligand and the water molecules in the MOF, whose relative strength and bond distances may slightly change when either Ni or Co ions are present in the framework. The existence of such a continuous evolution (rather than a random variation) of cell parameters with the composition is a clear indication in favor of the formation of a true solid solution. In particular, the *b* parameter increases continuously with the amount of Co in the bimetallic compound, while β follows the opposite trend. In contrast, parameters *a* and *c* follow a more complex evolution, with clear minima at around 33 mol% of Co.

The lack of a strict linearity of the cell parameters with composition indicates that the CoxNi-BTC compounds do not obey the Vegard's law[31]. This fact indicates that the distribution of

Co and Ni ions in the bimetallic compounds is not completely random. The presence of the minima in the curves of *a* and *c* at *ca*. 33 mol% Co strongly suggests a preferential occupation of the Co ions at the terminal positions, which are in a 1:2 multiplicity ratio with respect to bridging sites (see Fig. 3). This is a relevant observation, since if we assume that the terminal sites are preferentially occupied by Co^{2+} ions, rather than a random distribution of both elements, this would lead to a precise and predictable array of metal ions in the framework, which can be finely tuned by changing the overall composition of the bimetallic MOF. Thus, it should be possible to predict, to a certain extent, what would be the average separation between two closest Co ions as a function of the Co:Ni molar ratio of the solid, or to determine the probability to have an isolated Co^{2+}, surrounded only by Ni^{2+} ions in the closest positions. This certainly has important implications in the design and catalytic properties of well-defined single-site catalysts[2, 32], as we will illustrate in a forthcoming work.

It is worth mentioning that the addition of ethanol was found to be beneficial for the preparation of true solid solutions. Ethanol accelerates the overall precipitation process, which avoids the segregation of two pure phases of each individual monometallic MOF due to different rates of precipitation. Indeed, in the absence of ethanol, different precipitation rates were observed for pure Ni-BTC and Co-BTC monometallic compounds. Accordingly, when ethanol was not added to the synthesis mixture of bimetallic materials, incorporation of the two metals in the final compound was less quantitative (important deviations with respect to the ratio of precursors used) and varied from batch to batch, indicating that the crystallization process without ethanol is less homogeneous than when ethanol is added to the synthesis mixture.

To lend further support to the formation of solid solutions, we have slightly modified the synthesis conditions to obtain crystals suitable for single crystal diffraction (see Experimental section and Table S1 in the Supporting Information). Such large crystals (> 10 μm) were big enough for a complementary single crystal diffraction and SEM/EDX analysis. On one hand, single crystal diffraction confirmed the formation of the bimetallic compound with the same crystalline structure as the one obtained above[33]. On the other hand, EDX element mapping allowed us to conclude that both Ni and Co were simultaneously incorporated in a single particle and that they distribute homogeneously throughout the whole crystal; i.e., we did not detect Ni- or Co-enriched regions (such as tips or rims) in any of the single crystals analyzed. Fig. 5 shows typical SEM/EDX measurements obtained for samples containing 33% and 50% of cobalt, as representative examples

of the whole CoxNi-BTC series. The corresponding single crystal refinement for sample Co50Ni-BTC can be retrieved from the CIF file available in the Supporting Information.

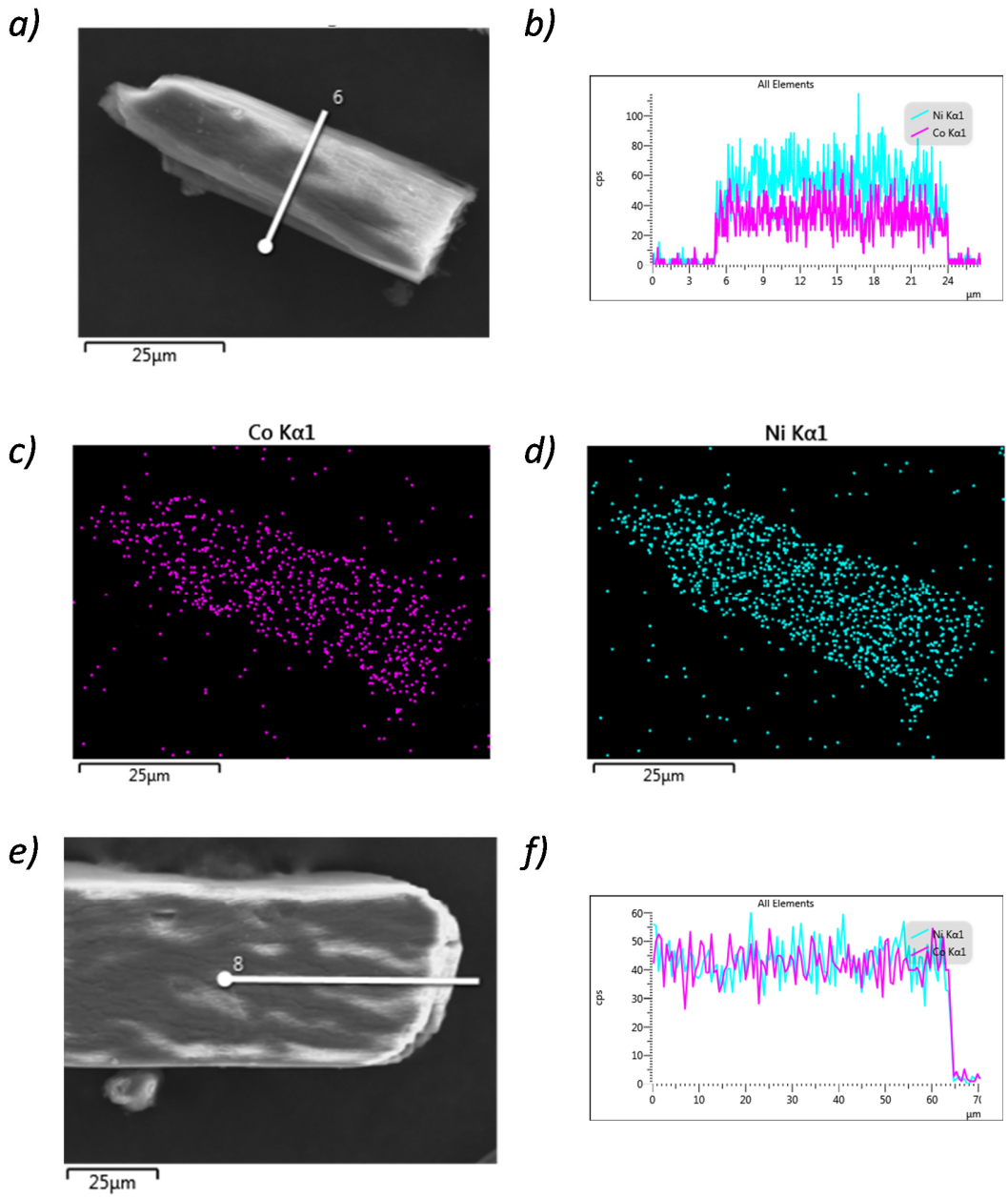

Figure 5. SEM/EDX analysis of samples Co33Ni-BTC (*a-d*) and Co50Ni-BTC (*e,f*) single crystal samples. *a*) and *e*): SEM images of the solids; *c*) and *d*): Co and Ni element mappings of the crystal shown in *a*); *b*) and *f*): Evolution of the Co (pink line) and Ni (cyan line) compositions along the white lines indicated in *a*) and *e*), respectively.

Co-Zn bimetallic compounds. The versatility and scope of the room temperature aqueous synthesis method described above was further investigated by preparing an additional series of Co-Zn bimetallic materials. The compounds were all found to be isoreticular in the complete range of compositions, as shown in Fig. S8 (Supporting Information). Also in this case, a continuous evolution of the cell parameters with the composition was clearly observed, but parameters *a* and *c* showed an opposite trend with respect to that observed for the Co-Ni series (see Fig. 4), with relative maxima (instead of minima) at *ca*. 30% Co, as shown in Fig. 6. In our opinion, the presence of these maxima in the evolution of *a* and *c* parameters reinforce the hypothesis that a preferred occupancy of the terminal positions by Co^{2+} ions occurs also in Co-Zn bimetallic mixtures. Meanwhile, parameters *b* and β followed a similar evolution with composition as that observed for Co-Ni mixtures: *i.e.*, *b* increases and β decreases with the Co content of the mixture.

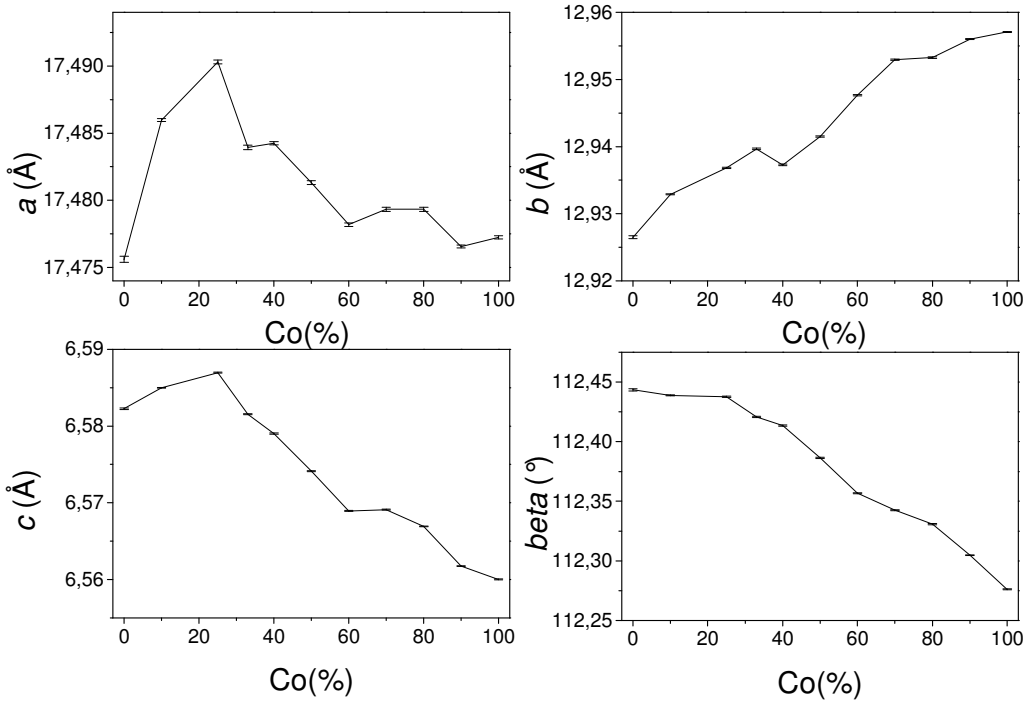

Figure 6. Variation of the cell parameters *a*, *b*, *c* and β, of bimetallic CoxZn-BTC compounds as a function of the molar composition.

Mn-Ni bimetallic compounds. In the course of an ongoing catalytic study of the M-BTC compounds (the results will be presented elsewhere), we were also interested in preparing Mn^{2+}-containing compounds having the same structure as the Co-BTC prepared herein. Unfortunately, as commented above, we have not been able to prepare a pure monometallic Mn-BTC isoreticular compound using the same aqueous synthesis procedure (see Fig. S1 in Supporting Information). Nevertheless, we succeeded in preparing a series of bimetallic compounds with the right structure containing Mn^{2+} ions in a Ni-BTC matrix up to a maximum concentration of 50% Mn, as shown in Fig. S9 (Supporting Information). Above this concentration of Mn^{2+} ions, bimetallic compounds showed a considerably lower crystallinity and the same (unknown) structure observed for the pure Mn-BTC compound.

The evolution of the cell parameters with the composition for the isoreticular MnxNi-BTC compounds, up to a maximum Mn content of 50%, is shown in Fig. 7. While parameters *b* and β follow the same general evolution already discussed for Co-Ni and Co-Zn compounds (*b* increases and β decreases with the Mn content), the continuous trends of the cell parameters *a* and *c* do not present any evident maxima or minima, but only a discontinuity in the trend of the *a* axis is observed at *ca*. 30-40% Mn. Unfortunately, our data in this case is not conclusive on whether a preferential site occupation or a random distribution of Mn^{2+} ions takes place.

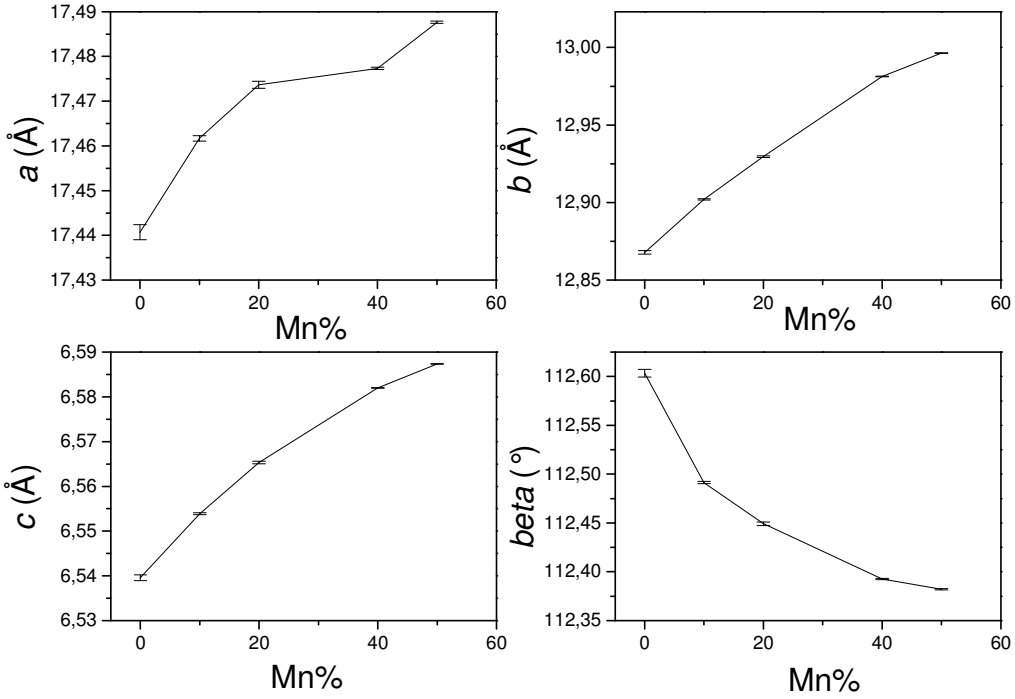

Figure 7. Variation of the cell parameters *a*, *b*, *c* and β, of bimetallic MnxNi-BTC compounds as a function of the molar composition.

CONCLUSIONS:

Herein we have applied a fast, sustainable and industrially friendly procedure for the synthesis of a series of isoreticular monometallic and bimetallic M-BTC compounds from aqueous solutions. These materials feature zigzag chains containing two positions for the metal ions; an unidentate bridging position (along the chain) and a bidentate terminal position (on alternate BTC molecules), in a 2:1 ratio. Packing of these chains into layers, and layer stacking lead to the three dimensional structure of the MOFs.

Following the synthesis method described here, we have been able to prepare isoreticular Co-Ni and Co-Zn binary mixtures in all range of compositions, as well as Mn-Ni compounds up to a maximum Mn concentration of 50%. By combining powder and single-crystal diffraction and SEM/EDX analysis of the solids, we have unambiguously demonstrated that true solid solutions are formed rather than physical mixtures, in which the two metal ions distribute homogeneously throughout the whole crystal (enrichment of one of the two metals at tips, rims or other regions of the crystal has never been observed in any of the analyzed samples). Moreover, a careful analysis

of the evolution of the cell parameters with the composition of Co-Ni and Co-Zn bimetallic compounds strongly suggests that a preferential occupation of the terminal positions by Co^{2+} ions takes place. If this is so, then the synthesis method used herein would lead to the formation of well-defined and predictable environments for the metal ions in the framework, which would basically depend upon the overall chemical composition of the binary materials. This would determine relevant parameters for the material properties, such as average distance between neighbor metal active sites or the statistical probability to have site isolation. Clear implications are envisaged for the final catalytic properties of bimetallic compounds, as we will demonstrate in a forthcoming report. As far as Mn-Ni mixtures is concerned, although preferential site occupation of terminal positions by Mn^{2+} ions is also feasible, our data are not conclusive enough to state it with certainty.

SUPPORTING INFORMATION

Specific conditions for the synthesis of bimetallic Co-Ni compounds; XRD of Co-BTC and Mn-BTC; TGA curves of monometallic M-BTC materials (M = Co, Ni, Cu, Zn); Measured weight losses and calculated molecular formula of the monometallic M-BTC compounds; Detailed view of hydrogen bond interactions between layers in M-BTC; XRD of bimetallic CoxNi-BTC compounds; Measured Co:Ni molar ratios in CoxNi-BTC compounds; Visual aspect of CoxNi-BTC compounds; Comparative TGA curves of bimetallic CoxNi-BTC and a physical mixture of Co-BTC + Ni-BTC; XRD of bimetallic CoxZn-BTC compounds; XRD of bimetallic MnxNi-BTC compounds

ACKNOWLEDGEMENTS:

This project has received funding from the European Union's Horizon 2020 research and innovation programme under the Marie Sklodowska-Curie grant agreement No. 641887 (project acronym: DEFNET) and the Spanish Government through projects MAT2017-82288-C2-1-P and Severo Ochoa (SEV-2016-0683). The Microscopy Service of the Universitat Politècnica de València is gratefully acknowledged for the electron microscopy measurements.

REFERENCES:

1. Corma, A.; Garcia, H.; Llabrés i Xamena, F. X., Engineering Metal Organic Frameworks for catalysis *Chem. Rev.* **2010,** *110*, 4606-4655, DOI: 10.1021/cr9003924.
2. Rogge, S. M. J.; Bavykina, A.; Hajek, J.; Garcia, H.; Olivos-Suarez, A. I.; Sepúlveda-Escribano, A.; Vimont, A.; Clet, G.; Bazin, P.; Kapteijn, F.; Daturi, M.; Ramos Fernandez, E. V.;

Llabrés i Xamena, F. X.; Van Speybroeck, V.; Gascon, J., Metal–organic and covalent organic frameworks as single-site catalysts. *Chem. Soc. Rev.* **2017,** *46*, 3134-3184, DOI: 10.1039/C7CS00033B.
3. Gascon, J.; Corma, A.; Kapteijn, F.; Llabrés i Xamena, F. X., Metal Organic Framework Catalysis: Quo vadis? *ACS Catal.* **2014,** *4*, 361-378, DOI: 10.1021/cs400959k.
4. Wang, Z. Q.; Cohen, S. M., Postsynthetic modification of metal-organic frameworks. *Chem. Soc. Rev.* **2009,** *38* (5), 1315-1329, DOI: 10.1039/B802258P.
5. Cavka, J. H.; Jakobsen, S.; Olsbye, U.; Guillou, N.; Lamberti, C.; Bordiga, S.; Lillerud, K. P., A New Zirconium Inorganic Building Brick Forming Metal Organic Frameworks with Exceptional Stability. *J. Am. Chem. Soc.* **2008,** *130*, 13850-13851, DOI: 10.1021/ja8057953.
6. Eddaoudi, M.; Kim, J.; Rosi, N.; Vodak, D.; Wachter, J.; O'Keeffe, M.; Yaghi, O. M., Systematic design of pore size and functionality in isoreticular MOFs and their application in methane storage. *Science* **2002,** *295*, 469-472, DOI: 10.1126/science.1067208.
7. Wade, C. R.; Dinca, M., Investigation of the Synthesis, Activation, and Isosteric Heats of CO2 Adsorption of the Isostructural Series of MOFs M3(BTC)2 (M=Cr,Fe,Ni,Cu,Mo,Ru). *Dalton Trans. 41*, 7931-7938, DOI: 10.1039/c2dt30372h.
8. Zou, R. Q.; Li, P. Z.; Zeng, Y. F.; Liu, J.; Zhao, R.; Duan, H.; Luo, Z.; Wang, J. G.; Zou, R.; Zhao, Y., Bimetallic Metal-Organic Frameworks: Probing the Lewis Acid Site for CO2 Conversion. *Small* **2016,** *12*, 2334-2343, DOI: 10.1002/smll.201503741.
9. Sun, D.; Sun, F.; Deng, X.; Li, Z., Mixed-Metal Strategy on Metal-Organic Frameworks (MOFs) for Functionalities Expansion: Co Substitution Induces Aerobic Oxidation of Cyclohexene over Inactive Ni-MOF-74. *Inorg. Chem.* **2015,** *54*, 8639-8643, DOI: 10.1021/acs.inorgchem.5b01278.
10. Aguirre-Díaz, L. M.; Gandara, F.; Iglesias, M.; Snejko, N.; Gutierrez-Puebla, E., Tunable Catalytic Activity of Solid Solution Metal–Organic Frameworks in One-Pot Multicomponent Reactions. *J. Am. Chem. Soc.* **2015,** *137*, 6132-6135, DOI: 10.1021/jacs.5b02313.
11. Zhang, J.; White, G. B.; Ryan, M. D.; Hunt, A. J.; Katz, M. J., Dihydrolevoglucosenone (Cyrene) As a Green Alternative to N,N -Dimethylformamide (DMF) in MOF Synthesis. *ACS Sust. Chem. Eng.* **2016,** *4*, 7186-7192, DOI: 10.1021/acssuschemeng.6b02115.
12. Reinsch, H., "Green" Synthesis of Metal-Organic Frameworks. *Eur. J. Inorg. Chem.* **2016,** *2016*, 4290-4299, DOI: 10.1002/ejic.201600286.
13. Julien, P. A.; Mottillo, C.; Friščić, T., Metal–organic frameworks meet scalable and sustainable synthesis. *Green Chem.* **2017,** *19*, 2729-2747, DOI: 10.1039/c7gc01078h.
14. Gaab, M.; Trukhan, N.; Maurer, S.; Gummaraju, R.; Müller, U., The progression of Al-based metal-organic frameworks – From academic research to industrial production and applications. *Microporous Mesoporous Mater.* **2012,** *157*, 131-136, DOI: 10.1016/j.micromeso.2011.08.016.
15. Chui, S. S. Y.; Lo, S. M. F.; Charmant, J. P. H.; Orpen, A. G.; Williams, I. D., A chemically functionalizable nanoporous material Cu-3(TMA)(2)(H2O)(3) (n). *Science* **1999,** *283* (5405), 1148-1150, DOI: 10.1126/science.283.5405.1148
16. Yuan, W. K.; Garay, A. L.; Pichon, A.; Clowes, R.; Wood, C. D.; Cooper, A. I.; James, S. L., Study of the Mechanochemical Formation and Resulting Properties of an Archetypal MOF: Cu3(BTC)2 (BTC = 1,3,5-Benzenetricarboxylate). *CrystEngComm* **2010,** *12*, 4063-4065, DOI: 10.1039/C0CE00486C.
17. Pichon, A.; Lazuen-Garay, A.; James, S. L., Solvent-free synthesis of a microporous metal–organic framework. *CrystEngComm* **2006,** *8*, 211-214, DOI: 10.1039/B513750K.

18. Klimakow, M.; Klobes, P.; Thünemann, A. F.; Rademann, K.; Emmerling, F., Mechanochemical Synthesis of Metal–Organic Frameworks: A Fast and Facile Approach toward Quantitative Yields and High Specific Surface Areas. *Chem. Mater.* **2010,** *22*, 5216-5221, DOI: 10.1021/cm1012119.
19. Stolar, T.; Batzdorf, L.; Lukin, S.; Zilic, D.; Motillo, C.; Friscic, T.; Emmerling, F.; Halasz, I.; Uzarevic, K., In Situ Monitoring of the Mechanosynthesis of the Archetypal Metal–Organic Framework HKUST-1: Effect of Liquid Additives on the Milling Reactivity. *Inorg. Chem.* **2017,** *56*, 6599-6608, DOI: 10.1021/acs.inorgchem.7b00707.
20. Friscic, T.; Jones, W., Recent Advances in Understanding the Mechanism of Cocrystal Formation via Grinding. *Cryst. Growth Des.* **2009,** *9*, 1621-1637, DOI: 10.1021/acs.inorgchem.7b00707.
21. Reinsch, H.; Waitschat, S.; Chavan, S.; Lillerud, K. P.; Stock, N., A Facile "Green" Route for Scalable Batch Production and Continuous Synthesis of Zirconium MOFs. *Eur. J. Inorg. Chem.* **2016,** *2016*, 4490-4498, DOI: 10.1002/ejic.201600295.
22. Petricek, V.; Dusek, M.; Palatinus, L., Crystallographic Computing System JANA2006: General Features. *Z. Kristallogr.* **2014,** *229*, 345-352, DOI: 10.1515/zkri-2014-1737.
23. Le Bail, A., Whole Powder Pattern Decomposition Methods and Applications: A Retrospection. *Powder Diffr.* **2005,** *20*, 316-326, DOI: 10.1154/1.2135315.
24. Rodriguez-Carvajal, J., Recent Advances in Magnetic Structure Determination by Neutron Powder Diffraction. *Physica B (Amsterdam)* **1993**, 55-69, DOI: 10.1016/0921-4526(93)90108-I.
25. Berar, J. F.; Lelann, P., E.s.d.'s and Estimated Probable Error Obtained in Rietveld Refinements with Local Correlations. *J. Appl. Crystallogr.* **1991,** *24*, 1-5, DOI: 10.1107/S0021889890008391.
26. Sheldrick, G. M., SHELXT – Integrated Space-Group and Crystal-Structure Determination. *Acta Crystallogr., Sect. A: Found. Crystallogr.* **2015,** *71*, 3-8, DOI: 10.1107/S2053273314026370.
27. Sheldrick, G. M., Crystal Structure Refinement with SHELXL. *Acta Crystallogr., Sect. C: Cryst. Struct. Commun.* **2015,** *71*, 3-8, DOI: 10.1107/S2053229614024218.
28. Dolomanov, O. V.; Bourhis, L. J.; Gildea, R. J.; Howard, J. A. K.; Puschmann, H., OLEX2: A Complete Structure Solution, Refinement and Analysis Program. *J. Appl. Crystallogr.* **2009,** *42*, 339-341, DOI: 10.1107/S0021889808042726.
29. Groom, C. R.; Bruno, I. J.; Lightfoot, M. P.; Ward, S. C., The Cambridge Structural Database. *Acta Crystallogr., Sect. B: Struct. Sci.* **2016,** *72*, 171-179, DOI: 10.1107/S2052520616003954
30. Yaghi, O. M.; Li, H.; Groy, T. L., Construction of Porous Solids from Hydrogen-Bonded Metal Complexes of 1,3,5-Benzenetricarboxylic Acid. *J. Am. Chem. Soc.* **1996,** *118*, 9096-9101, DOI: 10.1021/ja960746q.
31. Denton, A. R.; Ashcroft, N. W., Vegard's Law. *Phys. Rev. A* **1991,** *43*, 3161-3164, DOI: 10.1103/PhysRevA.43.3161.
32. Osad□hii, D. Y.; Olivos-Suarez, A. I.; Szé□sényi, A.; Li, G.; Nasalevi□h, M. A.; Dugulan, I. A.; Serra Crespo, P.; Hensen, E. J. M.; Veber, S. L.; Fedin, M. V.; Sankar, G.; Pidko, E. A.; Gascon, J., Isolated Fe Sites in Metal Organic Frameworks Catalyze the Direct Conversion of Methane to Methanol. *ACS Catal.* **2018,** *8*, 5542-5548, DOI: 10.1021/acscatal.8b00505.
33. , Unfortunately, single crystal diffraction analysis is not conlcusive on an eventual preferential occupation of the terminal sites by Co.

For Table of Contents Use Only

Facile "green" aqueous synthesis of mono- and bimetallic trimesate metal-organic frameworks

Anna Nowacka, Pol Briantais, Carmelo Prestipino and Francesc X. Llabrés i Xamena

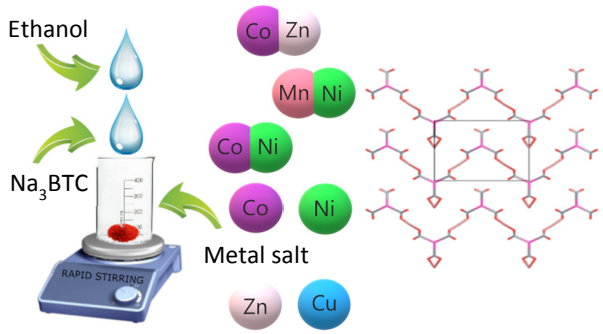

For Table of Contents Use Only

Synopsis

A facile, Green aqueous synthesis method is described leading to mono- and bimetallic MOFs having precise and predictable local environments